Journal of Inorganic Biochemistry 179 (2018) 146–153

Contents lists available at ScienceDirect

Journal of Inorganic Biochemistry

journal homepage: www.elsevier.com/locate/jinorgbio

# Photolabile ruthenium complexes to cage and release a highly cytotoxic anticancer agent☆

Jianhua Wei, Anna K. Renfrew*

*School of Chemistry, University of Sydney, Sydney, NSW, Australia*

ARTICLE INFO

*Keywords:*
Ruthenium
Prodrug
Drug delivery
Photocaging
Anticancer

ABSTRACT

CHS-828 (*N*-(6-(4-chlorophenoxy)hexyl)-*N′*-cyano-*N″*-4-pyridyl guanidine) is an anticancer agent with low bioavailability and high systemic toxicity. Here we present an approach to improve the therapeutic profile of the drug using photolabile ruthenium complexes to generate light-activated prodrugs of CHS-828. Both prodrug complexes are stable in the dark but release CHS-828 when irradiated with visible light. The complexes are water-soluble and accumulate in tumour cells in very high concentrations, predominantly in the mitochondria. Both prodrug complexes are significantly less cytotoxic than free CHS-828 in the dark but their toxicity increases up to 10-fold in combination with visible light. The cellular responses to light treatment are consistent with release of the cytotoxic CHS-828 ligand.

## 1. Introduction

The effectiveness of many anticancer agents can be compromised by factors such as systemic toxicity, low bioavailability, and metabolism. A prodrug approach can potentially circumvent these issues [1], where the drug is delivered in an inert, bioavailable form, then converted to the active form in the tumour region. Among the approaches under investigation for anticancer prodrug design, photocaging is gaining increasing interest as a means of selectively activating a prodrug in the tumour environment. In this strategy, a drug is 'caged' in an inactive form then 'uncaged' by irradiation with light [2]. The use of light as a trigger has the advantage of providing spatial and temporal control over the region of drug release, making this a potentially very selective means of prodrug activation. One key consideration is the irradiation wavelength, with 600–800 nm being the optimum window for maximum tissue penetration with minimum damage [3].

Ruthenium (II) polypyridyl complexes are particularly suited to photocaging as they can form stable complexes in the dark with a range of ligands, then undergo photosubstitution when irradiated with visible light [4]. Etchenique et al. first employed this approach in the photocaging of amine neurochemicals [5], while more recent work has focused on anticancer therapeutics, with pioneering work from Kodanko and Turro demonstrating photocaging of a nitrile-containing cathepsin K inhibitor [6]. We and others have subsequently expanded this approach to include imidazoles [7,8], and purines [9], with two very recent examples from Kodanko et al. focussing on pyridine-based drugs [10,11]. In this study we investigate the application of a photolabile ruthenium complex to cage and release a highly cytotoxic anticancer agent, CHS-828 (*N*-(6-(4-chlorophenoxy)hexyl)-*N′*-cyano-*N″*-4-pyridyl guanidine) (Fig. 1). This pyridine-containing compound is an inhibitor of the enzyme nicotinamide phosphoribosyltransferase (NAMPT) [12], which is overexpressed in a number of cancers [13]. CHS-828 exhibited potent antitumor activity in preclinical tumour models [14,15], and has subsequently completed several Phase I clinical trials against solid tumours [16–18]. However, in each trial the drug was found to induce a number of dose-limiting side effects such as gastrointestinal toxicity and thrombosis, in addition to low bioavailability and large variations in pharmacokinetics. Here we investigate whether incorporation of CHS-828 into two photolabile ruthenium complexes can improve upon these limitations.

## 2. Experimental

### 2.1. General procedures

#### 2.1.1. Materials

All other chemicals were obtained from commercial sources and used with further purification.

#### 2.1.2. Instrumentation and methods

$^1$H NMR spectra were collected at 300 K on a Bruker 300 MHz spectrometer using commercially available deuterated solvents.

☆ This paper is part of the AsiaBic8 Special Issue that appeared as Vol 177, Dec 2017, but was delayed in revision.

* Corresponding author.
*E-mail address:* anna.renfrew@sydney.edu.au (A.K. Renfrew).

https://doi.org/10.1016/j.jinorgbio.2017.11.018
Received 25 August 2017; Received in revised form 10 November 2017; Accepted 17 November 2017
Available online 22 November 2017

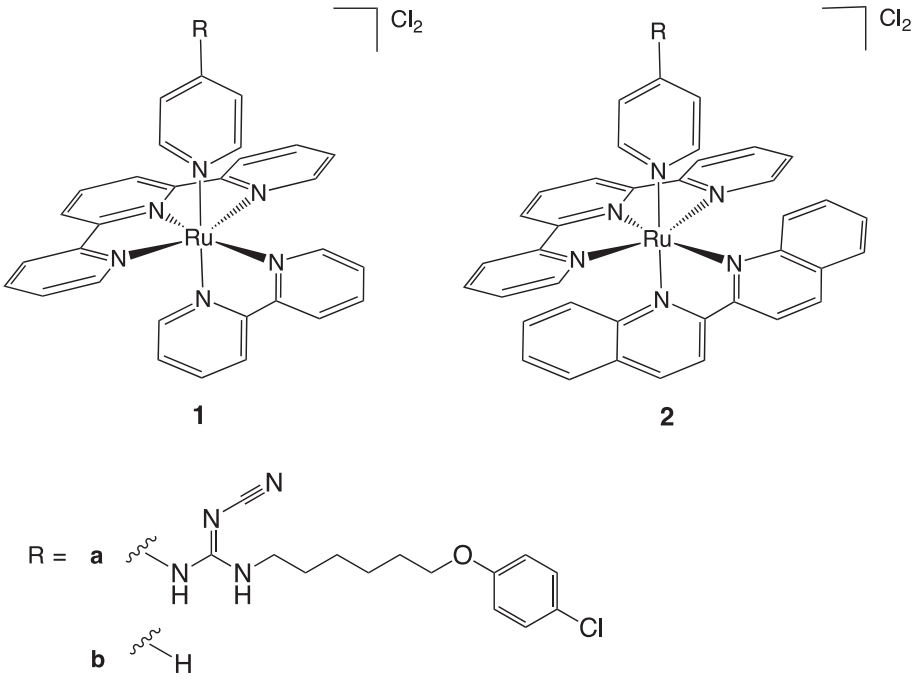


**Fig. 1.** Chemical structures of ruthenium complexes.

Isotopic impurities were used as internal reference signals. Mass spectrometry was performed using Electro-Spray Ionisation using an amazon SL spectrometer. Elemental analyses (C, H, N) were conducted by the Chemical & MicroAnalytical Services Pty Ltd., Campbell Microanalytical Laboratory, at the University of Otago. ICPMS was conducted at the National Measurements Institute, Pymble, NSW, Australia. UV–visible measurements were performed on a Cary 4E UV–visible spectrometer using a 1 cm × 1 cm quartz cuvette.

Scans were run at room temperature from 300 to 700 nm.

### 2.2. Synthesis

CHS-828 [12], [Ru(tpy)(bpy)Cl]Cl (tpy = 2,2′;6′,2″-terpyridine), (bpy = 2,2′-bipyridine) [19], [Ru(tpy)(biq)Cl]Cl (biq = (2,2′-biquinoline) [19], $[Ru(tpy)(bpy)(py)]Cl_2$ (py = pyridine) [20], $[Ru(tpy)(biq)(py)]Cl_2$ [20] were prepared according to literature procedures.

All reactions were carried out under nitrogen using standard Schlenk techniques. The synthesis and purification of the final complexes were performed under low ambient light to avoid photodegradation.

$[Ru(tpy)(bpy)(CHS-828)]Cl_2$ (1a)

A solution of [Ru(tpy)(bpy)Cl]Cl (263 mg, 0.5 mmol) in 1:3 water/MeOH (40 mL) was heated at reflux for 30 min in the absence of light. CHS-828 (222 mg, 0.6 mmol) was added and the reaction heated at reflux for further 12 h, then the solvent removed under reduced pressure. The residue was purified by column chromatography on an alumina column (neutral, Brockmann activity 3) with a gradient eluent of dichloromethane:MeOH (10:1 to 2:1). Residual [Ru(tpy)(bpy)Cl]Cl elutes first as a pink band followed by Complex (1a) as an brown band. The fractions were combined, concentrated and precipitated with diethyl ether to give a red/brown powder, which was collected by filtration, washed with diethyl ether (2 × 20 mL) and dried under vacuum. Final yield of Complex (1a) = 288 mg (62%) of red/brown microcrystals.

$^1$H NMR (300 MHz, Methanol-$d_4$) 9.51 (1H, d, $J$ 5.5), 8.78 (1H, d, $J$ 8.2), 8.66 (2H, d, $J$ 8.1), 8.53 (3H, d, $J$ 8.0), 8.34 (1H, t, $J$ 7.8), 8.26 (1H, t, $J$ 8.0), 8.02 (2H, d, $J$ 7.6), 7.99–7.90 (3H, m), 7.80 (1H, t, $J$ 7.9), 7.60 (2H, d, $J$ 5.5), 7.37 (2H, t, $J$ 6.6), 7.29 (1H, d, $J$ 5.6), 7.21 (2H, d, $J$ 8.6), 7.10 (1H, t, $J$ 6.7), 6.85 (2H, d, $J$ 8.4), 6.65 (2H, d, $J$ 5.7), 3.90 (2H, t, $J$ 6.3), 3.31 (1H, s), 3.12 (2H, t, $J$ 6.9), 1.75–1.63 (2H, m), 1.42 (4H, p, $J$ 7.5), 1.30 (3H, q, $J$ 8.0, 7.5). ESI-MS +: $m/z$ = 431.17 ($[Ru(tpy)(bpy)(CHS-828)])^{2+}$, 861.24 ($[Ru(tpy)(bpy)(CHS-828)]$-H)$^+$. Elemental analysis for $[Ru(tpy)(bpy)(CHS-828)](Cl)_2(H_2O)_2(CH_3OH)$ ($C_{45}H_{49}Cl_3N_{10}O_4Ru$). Calculated: C, 53.98; H, 4.93; N, 13.99. Found: C, 53.69; H, 4.94; N, 13.90.

$[Ru(tpy)(biq)(CHS-828)]Cl_2$ (2a)

A solution of [Ru(tpy)(biq)Cl]Cl (313 mg, 0.5 mmol) in 1:3 water/MeOH (40 mL) was heated at reflux for 30 min in the absence of light. CHS-828 (222 mg, 0.6 mmol) was added and the reaction heated at reflux for further 12 h, then the solvent removed under reduced pressure. The residue was purified by column chromatography on an alumina column (neutral, Brockmann activity 3) with a gradient eluent of dichloromethane:MeOH (10:1 to 2:1). Residual [Ru(tpy)(biq)Cl]Cl elutes first as a bright pink band followed by Complex (2a) as an purple band. The fractions were combined, concentrated and precipitated with diethyl ether to give purple crystalline solid, which was collected by filtration, washed with diethyl ether (2 × 20 mL) and dried under vacuum. Final yield of Complex (2a) = 299 mg (58%) of purple microcrystals.

$^1$H NMR (300 MHz, Methanol-$d_4$) 9.03 (1H, q, $J$ 8.9), 8.88 (1H, d, $J$ 8.2), 8.77 (1H, d, $J$ 8.5), 8.70 (1H, d, $J$ 8.1), 8.52 (1H, d, $J$ 8.0), 8.41 (2H, t, $J$ 8.6), 8.34 (1H, t, $J$ 8.0), 8.09–7.87 (4H, m), 7.86 (1H, d, $J$ 8.1), 7.72 (1H, d, $J$ 5.6), 7.49 (2H, t, $J$ 7.5), 7.38 (1H, td, $J$ 6.1, 5.7, 3.0), 7.22 (3H, dd, $J$ 8.7, 5.7), 6.87 (2H, d, $J$ 9.0), 6.76 (1H, d, $J$ 8.8), 6.57 (1H, d, $J$ 9.8), 4.00–3.82 (3H, m), 3.15–2.97 (2H, m), 1.70 (2H, t, $J$ 7.3), 1.41 (5H, s), 1.29 (2H, d, $J$ 9.8). ESI-MS +: $m/z$ = 481.93 ($[Ru(tpy)(biq)(CHS-828)])^{2+}$, 961.18 ($[Ru(tpy)(biq)(CHS-828)]$-H)$^+$.

Elemental analysis for $[Ru(tpy)(biq)(CHS-828)](Cl)_2(CH_3OH)_4$ ($C_{56}H_{61}Cl_3N_{10}O_5Ru$). Calculated: C, 57.90; H, 5.29; N, 12.06. Found: C, 58.13; H, 5.25; N, 12.04.

### 2.3. Spectroscopic studies

Solutions of the ruthenium complexes in water were prepared in a quartz cuvette to give a final concentration of 50 μM. Solutions prepared in methanol or DMSO and diluted with water to give a final composition of 95:1 water/methanol or water/DMSO. The cuvette was irradiated with an LED-EXPO lamp (LuzChem) at 465 ± 10 nm,

520 ± 10 nm or 590 ± 10 nm, at 2.5 mW.cm$^{-2}$. UV–visible absorbance spectra were recorded at regular intervals and ESI mass spectra of the initial and final solutions were collected. The half-lives of photoinduced ligand exchange were determined by fitting the decrease in absorbance maxima against time to a first order exponential decay using Prism 6 Software. The quantum yield for photoinduced ligand exchange was determined as reported previously [7] by monitoring the decrease in absorbance maxima as a function of irradiation time. Ferrioxalate actinometry was used to determine the photon flux of the LED light source [21]. The quantum yield of photolysis was determined by plotting the decrease in the number of moles of complex per unit time (determined from the UV–visible absorbance maxima by $c = A / \varepsilon l$) against the number of moles of photons during the initial 20% of the photoreaction. The slope of the plot gives the quantum yield.

### 2.4. Biological studies

#### 2.4.1. Cell lines

A549 human lung carcinoma, and MCF-7 human breast carcinoma cells were purchased from ATCC and used within 2 months of resuscitation. Cells were maintained in Advanced DMEM (Dulbecco's Modified Eagle's Medium) (Invitrogen) and supplemented with 2% FBS (fetal bovine serum) and 2 mM glutamine in a humidified environment at 37 °C and 5% $CO_2$.

#### 2.4.2. Ruthenium accumulation

2 million A549 cells in 10 mL of advanced DMEM were seeded in a 10 cm dish and allowed to adhere overnight. The media was replaced and the cells treated with 20 μM of Complexes (1a), (1b), (2a) or (2b) in DMSO (dimethyl sulfoxide) (final DMSO concentration = 0.4%). Following incubation for 4 h, the media was removed, the cells trypsinized and 5 mL of PBS (phosphate-buffered saline) solution added. The cells were centrifuged at 2000 rpm for 4 mins, the supernatant removed and the process repeated 3 times. The pellet was then resuspended in 0.5 mL of PBS solution. Ruthenium concentrations were determined by ICPMS (Inductively-Coupled Plasma Mass Spectrometry) using a NexION300 (PerkinElmer). Samples were digested with 15 M nitric acid prior to analysis. Cellular concentrations of ruthenium were reported per mg of protein. Bio-rad protein assay dye was diluted five-fold with double distilled water and then 200 μL of the diluted reagent was added to each well of a 96-well plate. Using a 1 mg mL$^{-1}$ solution of bovine serum albumin in PBS, protein standards of concentrations 500, 250, 125, 62.5, 31.3 and 15.6 μg mL$^{-1}$ were prepared. Cellular samples were diluted by a factor of 10 before a 10 μL aliquot was added to each well containing the diluted dye reagent. The protein/dye mixtures were left for 1 h before absorbance at 600 nm was determined using a Victor3V microplate reader.

#### 2.4.3. Subcellular ruthenium accumulation

2 million A549 cells in 10 mL of advanced DMEM were seeded in a 10 cm dish and allowed to adhere overnight. The media was replaced and the cells treated with 20 μM of Complexes (1a) and (2a) in DMSO (final DMSO concentration = 0.4%). Following incubation for 4 h, the media was removed, the cells trypsinized and 5 mL of PBS solution added. The cells were centrifuged at 2000 rpm for 4 mins, the supernatant removed and the process repeated 3 times. Cell pellets were fractionated using the Cell FractionPREP kit (including cytosol, nucleus, membrane/particulate and cytoskeletal fractions), Mitochondria isolation kit, and Genomic DNA isolation kit from BioVision according to the supplier's instructions. Ruthenium concentrations were determined by ICPMS using a NexION300 (PerkinElmer). Samples were digested with 15 M nitric acid prior to analysis. Concentrations of ruthenium were reported per mg of protein. Bio-rad protein assay dye was diluted five-fold with double distilled water and then 200 μL of the diluted reagent was added to each well of a 96-well plate. Using a 1 mg mL$^{-1}$ solution of bovine serum albumin in PBS, protein standards of concentrations 200, 160, 120, 80, 60, 40 and 20 μg mL$^{-1}$ were prepared. Cellular samples were diluted by a factor of 10 before a 10 μL aliquot was added to each well containing the diluted dye reagent. The protein/dye mixtures were left for 1 h before absorbance at 600 nm was determined using a Victor3V microplate reader.

#### 2.4.4. Photocytotoxicity assay

Cytotoxicity was determined using the MTT (3-(4,5-Dimethylthiazol-2-yl)-2,5-Diphenyltetrazolium Bromide) assay. $2 \times 10^3$ A549 or $1 \times 10$ [4] MCF-7 cells per well were plated on to 96-well plates and allowed to adhere overnight. Freshly prepared media/DMSO (90:10) solutions of the complexes and CHS-828 were added to triplicate wells at concentrations spanning a 4-log range (final DMSO concentrations < 0.5%) and incubated in the dark for 4 h. The media was removed and replaced with phenol red free DMEM (Invitrogen) (100 μL per well) and the cells irradiated for 30 min (corresponding to a light dose of 8.5 J cm$^{-2}$) with an LED-EXPO lamp (LuzChem) (λLED = 465 nm), or incubated in dark for the same time period. The phenol red free DMEM was removed and replaced with advanced DMEM and the cells incubated in the dark for a further 96 h, following which, 3-(4,5-Dimethylthiazol-2-yl)-2,5-diphenyltetrazolium bromide (1.0 mM) was added to each well and the cells incubated for 4 h. The culture medium was removed and the resulting purple precipitate dissolved in DMSO (100 μL). The absorbance measured at 600 nm using a Victor3V microplate reader (Perkin Elmer). At least three independent experiments were performed for each compound with triplicate readings in each experiment. $IC_{50}$ values were determined as the drug concentrations required to reduce the absorbance to 50% of that of the untreated control wells. The viability of untreated control cells was determined with and without light irradiation to establish the effect of the green light. The viability of A549 cells was not affected by the light treatment alone but MCF-7 cells showed up to 10% decrease in viability under the same conditions. To remove possible effects of the light treatment, all $IC_{50}$ values were determined relative to the viability of the appropriate light or dark control cells. $IC_{50}$ values were calculated by fitting the data to a sigmoidal dose response curve using GraphPad Prism 7 Software.

#### 2.4.5. DNA unwinding

For plasmid DNA unwinding experiments, supercoiled pBR322 DNA (0.5 μg) was treated with different concentration of CHS828, Complexes (1a) and (2a) (2, 10 μM) in the TBE buffer (TBE: Tris-Boric acid-EDTA buffer solution). The light samples were irradiated for 15 min before being incubated at 37 °C in dark for 2 h. All samples were analysed by electrophoresis for 2 h at 70 V in the TBE buffer. The gel was then stained by EB (Ethidium Bromide) for 20 min and visualized and photographed via a BIO-RAD imaging system under a UV–Vis transilluminator.

#### 2.4.6. Measurement of intracellular ROS production

$1 \times 10$ [4] A549 cells were plated on to 2 mL Matek dishes and allowed to adhere overnight, then incubated with 1 μM of Complexes (1a), (2a) or CHS-828 in the dark for 4 h. For the dark samples, the media was replaced with phenol red free DMEM and the cells were incubated with 20 μM H2DCFDA (2′,7′-Dichlorodihydrofluorescein diacetate) (Sigma-Aldrich) for 30 min at 37 °C. The light samples were irradiated for 30 min as described above, following which, the media was replaced with fresh phenol red free DMEM and the cells were incubated with 20 μM H2DCFDA for 30 min at 37 °C. The media was removed and replaced with fresh phenol red free DMEM and the cells imaged directly on a Nikon Ti-S microscope with a C-FL Epi-Fl Filter Cube N B-2A excitation 450–490 nm and emission at 520 nm. Three independent experiments were performed for each treatment. Quantification of the fluorescence intensity was carried out using nis-element D by drawing a 20 μm [2] square over a representative portion of the image and measuring the integrated fluorescence intensity.

Measurements were taken from at least 5 different images in each treatment group.

#### 2.4.7. Measurement of mitochondrial membrane potential

$1 \times 10$ [4] A549 cells were plated on to 2 mL Matek dishes and allowed to adhere overnight, then incubated with 1 μM of Complexes (1a), (2a) or CHS-828 in the dark for 4 h. The media was removed and replaced with phenol red free DMEM (Invitrogen) and the cells irradiated for 30 min or incubated in dark for the same time period. The phenol red free DMEM was removed and replaced with advanced DMEM and the cells incubated in the dark for further 24 h. Cells were loaded with 10 μg $mL^{-1}$ J $C^{-1}$ dye for 30 min at 37 °C. The media was removed and cells were washed with fresh PBS three times. The plate was imaged with a Nikon Ti-s microscope with a C-FL Epi-Fl Filter Cube N B-2A excitation 450-490 nm and emission at 520 nm (green fluorescence, monomers) and with a C-FL Epi-Fl Filter Cube N G-2A excitation 510-560 nm and emission at 590 nm (red fluorescence, aggregates), respectively. Three independent experiments were performed for each treatment. Quantification of the fluorescence intensity was carried out using nis-element D by drawing a 100 μm [2] square over a representative portion of the image and measuring the integrated fluorescence intensity. Measurements were taken from at least 5 different images in each treatment group.

## 3. Results and discussion

### 3.1. Synthesis

$[Ru(tpy)(bpy)(CHS\text{-}828)]Cl_2$ (Complex (1a)) and $[Ru(tpy)(biq)(CHS\text{-}828)]Cl_2$ (Complex (2a)) were prepared by refluxing the appropriate chlorido complexes ($[Ru(tpy)(N\text{-}N)Cl]Cl$) with a slight excess of CHS-828 in methanol/water. Purification on an alumina column gave the pure complexes in ca. 60% yield. The complexes were characterised by $^1H$ NMR and UV–visible absorbance spectroscopy, ESI-mass spectrometry and elemental analysis. In each case the mass spectra show both the $[M]^{2+}$ parent ion and $[M\text{-}H]^+$ ion, most likely due to deprotonation of the cyanguanidine moiety on the CHS-828 ligand. The $^1H$ NMR spectra show a significant upfield shifting of the CHS-828 pyridine signals relative to the phenol signals, indicative of ruthenium binding to the pyridine nitrogen. This observation is supported by the UV–visible absorbance spectra where each complex has a broad MLCT band, at 470 nm (Complex (1a)) and 538 nm (Complex (2a)), respectively (Table 1). The spectra are very similar to the analogous pyridine complexes [20] Complex (1b) and (2b) (Fig. S3), though the absorbance maxima are slightly red-shifted in the CHS-828 complexes, most likely due to the cyanoguanidine group in the *para* position of the CHS-828 ligand.

### 3.2. Stability and photostability in solution

Complexes (1a) and (2a) are soluble in water, and freely soluble in methanol and acetonitrile. Notably, CHS-828 itself is highly insoluble in water and most polar organic solvents, which has been linked to its low bioavailability in vivo [22]. Both complexes demonstrate high stability in water/DMSO solutions in the dark, with no change in the UV–visible absorbance spectra observed after 24 h (Fig. S3). In contrast, irradiation of aqueous solutions of Complex (1a) or (2a) with blue light (465 nm) results in a clear decrease in the original absorbance band, concurrent with the formation of a new, lower energy band (Fig. 2). In each case the absorbance maxima of the new band is consistent with the formation of the aqua complex $[Ru(tpy)bpy(H_2O)]^{2+}$ ($\lambda_{max}$ = 480 nm) or $[Ru(tpy)(biq)(H_2O)]^{2+}$ ($\lambda_{max}$ = 548 nm) [20]. Clear isosbestic points indicate that this is a single step reaction, with the ESI mass spectra of irradiated samples revealing the only products to be a solvent bound ruthenium complex, $[Ru(tpy)(L)(S)]^{2+}$ and free CHS-828, $[M\text{-}H]^-$ (Figs. S2c and S2d).

**Table 1**
Absorbance maxima, extinction coefficients, half-lives and quantum yields of ligand release in water.

| | $\lambda_{max}$ (nm) (ε ($M^{-1}$ $cm^{-1}$)) | $t_{1/2}$ (min) $\lambda_{465}$ | Φ (%) $\lambda_{465}$ | $t_{1/2}$ (min) $\lambda_{520}$ | $t_{1/2}$ (min) $\lambda_{590}$ |
|---|---|---|---|---|---|
| Complex (1a) | 470 (8259) | 40 | 0.11 | | |
| Complex (1b) | 468 (8674) | 16.7 | 0.01 | | |
| Complex (2a) | 538 (7820) | 3.3 | 0.38 | 8.8 | 24.59 |
| Complex (2b) | 531 (8210) | 1.8 | 1.3 | – | – |

The quantum yield of ligand release from Complex (2a) was found to be ca. 3-fold lower than the analogous pyridine complex $[Ru(tpy)(biq)(py)]Cl_2$ (Complex (2b)) (Table 1). This may be due to the influence of the *para*-cyanoguanidine substituent on the pyridine ring. Alternatively, the low solubility of CHS-828 may reduce the rate of ligand exchange as it is harder for the ligand to escape the solvent cage. Release of CHS-828 could also be achieved from Complex (2a) at longer irradiation wavelengths of 520 and 590 nm (Fig. S4). While photo-induced ligand release was slower under these conditions, the possibility of triggering drug release at these longer wavelengths greatly increases the scope of this complex to treat deeper within tissue. In agreement with previous findings [20], the bipyridine Complexes (1a) and (1b) have much lower quantum yields of ligand release than their biquinoline analogues. Despite the slow rate of photo-induced ligand exchange, a significant concentration of CHS-828 can be released from both Complexes (1a) and (2a) with relatively low doses of light ($t_{1/2}$ Complex (1a) = 40 min irradiation = 11.3 J $cm^{-2}$) that are suitable for in vitro cell culture experiments.

### 3.3. Intracellular ruthenium concentration

To effectively deliver CHS-828, the ruthenium complexes must be able to accumulate in tumour cells in reasonable concentrations. The intracellular ruthenium concentrations of A549 cells treated with Complexes (1a), (1b), (2a), and (2b) were determined by ICPMS and are reported as ng of ruthenium per mg of cellular protein in Fig. 3. The CHS-828 ligand was found to markedly enhance cellular uptake: cells treated with Complexes (1a) and (2a) had intracellular ruthenium levels 20-fold higher than those treated with (1b) and (2b), respectively. This can be attributed to the significantly higher lipophilicity of CHS-828 (logP = 3.98, vs. -0.4 for pyridine). These intracellular ruthenium levels are among the highest reported [23–25], which is noteworthy considering that Complexes (1a) and (2a) are also soluble in water. While ICPMS does not give information on the speciation of the ruthenium complex, this marked difference in accumulation suggests that the CHS-828 ligand remains coordinated. This is further supported by the observation that the aqua complex $[Ru(tpy)(bpy)(OH_2)]^{2+}$ has very poor cellular accumulation [26].

### 3.4. Subcellular ruthenium accumulation

In order to obtain more detailed information on the localisation of ruthenium within the cell, the concentration of ruthenium in the nucleus, mitochondria, cytosol, cytoskeleton and membrane were determined by ICPMS (Fig. 3). In addition to good cellular uptake, the ability of the complexes to deliver CHS-828 to its cellular target, NAMPT, is an important consideration. NAMPT is located in the cell cytoplasm, nucleus and mitochondria [13] but to the best of our knowledge it is not known whether CHS-828 binds to NAMPT in a specific organelle or in all of these regions. For both Complexes (1a) and (2a), the majority of ruthenium is localised in the mitochondria (70% and 61% for Complexes (1a) and (2a), respectively), with approximately 5% in the cell nucleus and 8% in the cytoplasm. A greater proportion of Complex (2a) is found in the cell membrane and cytoskeleton, which can be attributed to its higher lipophilicity.

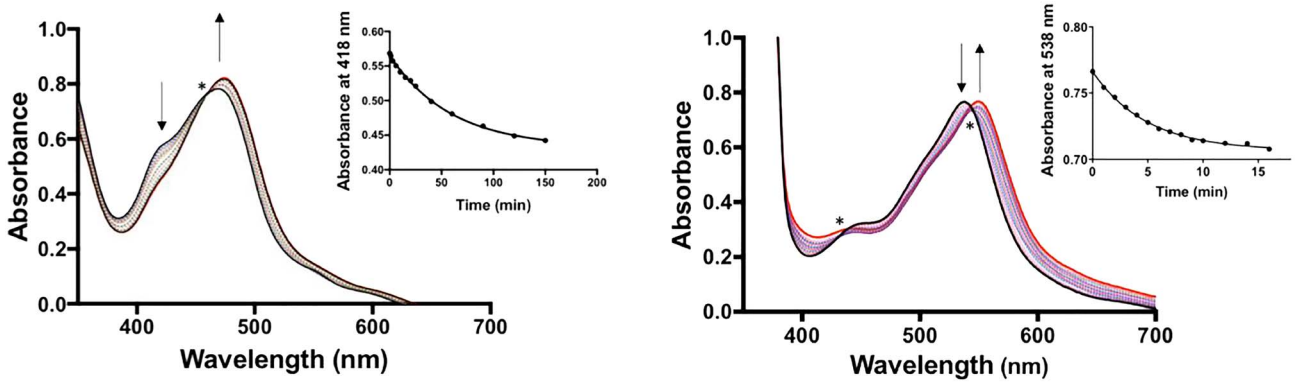


**Fig. 2.** Aqueous solution of Complex (1a) (left) and Complex (2a) (right) irradiated with blue light. (For interpretation of the references to colour in this figure legend, the reader is referred to the web version of this article.)

### 3.5. Photocytotoxicity

Having established that the CHS-828 prodrugs (1a) and (2a) can accumulate in cells in high concentrations, the cytotoxicity and photocytotoxicity of all complexes and CHS-828 was evaluated against A549 and MCF-7 cells. These cell lines were chosen as they are known to be sensitive to CHS-828 [27]. Cells were dosed with the compounds for 4 h, then the media replaced and the cells either irradiated with blue light for 30 min (final dose = 8.5 J $cm^{-2}$) or kept in the dark for the same time period. The cells were then incubated for a further 96 h and the viability determined using the MTT assay. Cell viability plots (determined relative to the dark or light-treated control cells) are shown in Figs. 4, S6 and S7, and $IC_{50}$ values reported in Table 2.

In agreement with previous findings [27], CHS-828 showed very high cytotoxicity towards both cell lines, with $IC_{50}$ values of 13 and 79 nM, respectively. It should be noted that these $IC_{50}$ values are higher than those previously reported in the same cell lines due to the shorter dosing time used in this experiment (4 h vs. 96 h). Irradiation with light did not significantly affect the viability of cells treated with CHS-828.

Complexes (1a) and (2a) were found to be markedly less cytotoxic in the dark than CHS-828, with $IC_{50}$ values ca. 70-fold lower for Complex (1a) and 25–50 fold lower for Complex (2a), though the $IC_{50}$ values of the complexes are still relatively low (0.3–5.8 μM). On irradiation with light, the complexes are significantly more cytotoxic towards both cell lines: in particular Complex (1a) shows a 10-fold increase in toxicity. This is comparable to the photoselectively index of Photofrin, a clinically approved photosensitiser [28]. Despite the low efficiency of light-induced CHS-828 release from Complex (1a), the complex offers good selectivity between dark and light-treated cells. It should be noted that the half-life of ligand release for Complex (1a) is 40 min in water (Table 1), therefore 30 min of irradiation would be expected induce the release of a significant concentration of CHS-828. From the photostability studies in solution, Complex (2a) would have been expected to give the most efficient release of CHS-828 and hence a larger photoselectivity index than Complex (1a). It is not clear why the photoselectivity index of Complex (2a) is 2-fold lower than Complex (1a) but this may be due to the difference in subcellular ruthenium distribution:

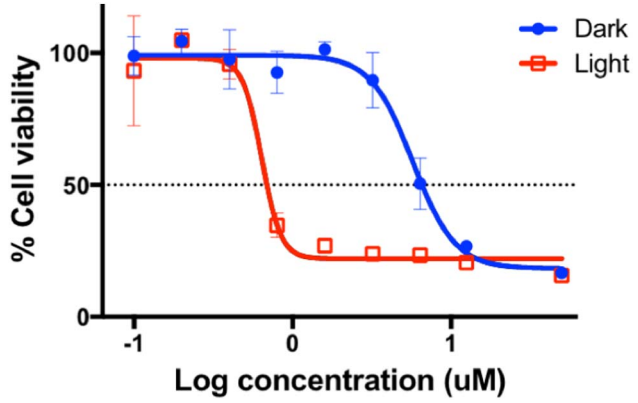


**Fig. 4.** Sigmoidal fits of dose response curves for MCF-7 cells treated with Complex (1a).

**Table 2**
$IC_{50}$ values (nM) in A549 and MCF-7 cells. The cells were incubated in the dark or irradiated with blue light for 30 min (dose = 8.5 J $cm^{-2}$).

| | $IC_{50}$ A549 (nM) dark | $IC_{50}$ A549 (nM) light | PI[a] | $IC_{50}$ MCF-7 (nM) dark | $IC_{50}$ MCF-7 (nM) light | PI |
|---|---|---|---|---|---|---|
| CHS-828 | 13 ± 2 | 11 ± 1 | 1.2 | 79 ± 10 | 100 ± 20 | 0.8 |
| Complex (1a) | 800 ± 20 | 84 ± 20 | 9.5 | 5800 ± 800 | 570 ± 70 | 10.2 |
| Complex (2a) | 300 ± 40 | 68 ± 7 | 4.4 | 3900 ± 50 | 860 ± 100 | 4.5 |
| Complex (1b) | > 50,000 | > 50,000 | – | > 50,000 | > 50,000 | – |
| Complex (2b) | > 50,000 | > 50,000 | – | > 50,000 | > 50,000 | – |

[a] PI = Photoselectivity index (Dark $IC_{50}$ / Light $IC_{50}$)

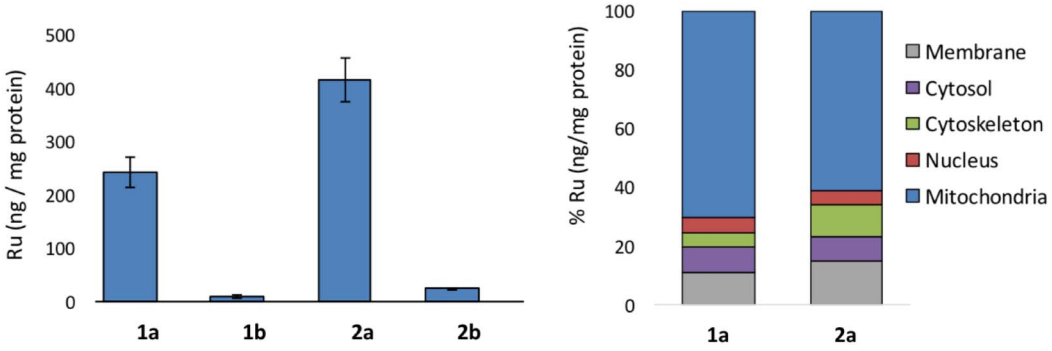


**Fig. 3.** Intracellular ruthenium concentrations (ng/mg protein) in whole cells (left) and cellular fractions (right).

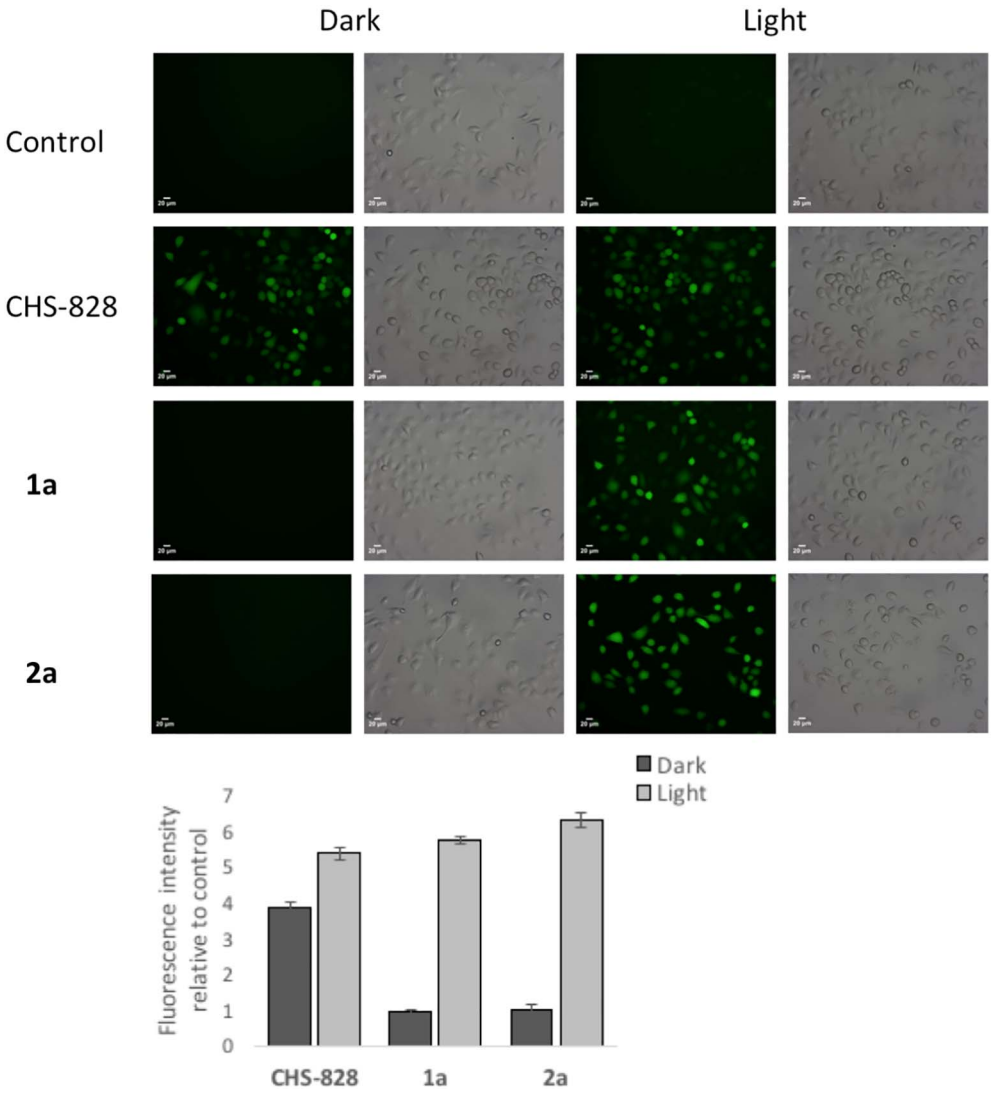


**Fig. 5.** Measurement of ROS production. Mean fluorescence intensities relative to untreated control cells of A549 cells treated with H2DCFDA after incubation with CHS-828, Complex (1a) or (2a) for 4 h. Scale bar = 20 μm.

a relatively larger percentage of Complex (1a) accumulates in the mitochondria, with a relatively larger percentage of Complex (2a) in the membrane and cytoskeleton.

This increase in cytotoxicity for both complexes on irradiation is consistent with light-triggered release of the highly cytotoxic ligand, CHS-828, however it is also possible that photosubstitution produces a cytotoxic ruthenium complex. To further investigate this possibility, the photocytotoxicity of the pyridine analogues Complexes (1b) and (2b) was also evaluated. Neither complex is cytotoxic towards the two cell lines tested in the dark or in combination with light ($IC_{50} \geq 50$ μM), however the significantly lower levels of cellular accumulation make it difficult to directly compare the pyridine complexes with their CHS-828 analogues. Kodanko et al. recently reported an analogue of Complex (2a) with a lipophilic pyridine ligand, Abiraterone (log-$P_{Abiraterone} = 3.97$), that produces the same ruthenium photoproduct on irradiation [11]. Neither the free ligand, nor the complex in combination with light are significantly toxic towards DU145 cells below a concentration of 20 μM, suggesting that light irradiation does not produce a highly cytotoxic complex.

### 3.6. DNA binding

To further probe the mechanism of light-induced toxicity for Complexes (1a) and (2a), a number of cellular responses were studied and compared to those of cells treated with free CHS-828. While Complexes (1a) and (2a) predominantly accumulate in the mitochondria, there is still a considerable fraction of ruthenium in the nucleus (5%). DNA has been identified as a target for many ruthenium (II) polypyridyl complexes, where covalent binding or intercalation leads to cross linking or strand cleavage [29]. The ability of the CHS-828 complexes to bind to or damage DNA was evaluated by gel electrophoresis. CHS-828, Complex (1a), and Complex (2a), were incubated with pBR322 plasmid DNA and irradiated with blue light for 15 min or kept in the dark (Fig. S8). In each case, the treated DNA samples showed the same retention as the control, suggesting that the complexes do not nick, intercalate with DNA, or induce cross-linking.

### 3.7. ROS production

Inhibition of NAMPT by CHS-828 has previously been reported to increase ROS production by depleting NAD + [30]. Cellular ROS levels were measured in A549 cells treated with CHS-828, Complex (1a), and Complex (2a) using the using the nonfluorescent dye, H2DCFDA, which is converted to fluorescent DCF in the presence of ROS. A549 cells were treated with the compounds and incubated for 4 h, then the media was replaced and cells were either irradiated with blue light or incubated in the dark for 30 min prior to addition of H2DCFDA. The fluorescence intensities determined by confocal fluorescence microscopy are shown in Fig. 5. In agreement with previous studies, ROS levels of cells treated with CHS-828 are 4–5 fold greater than those of the untreated control

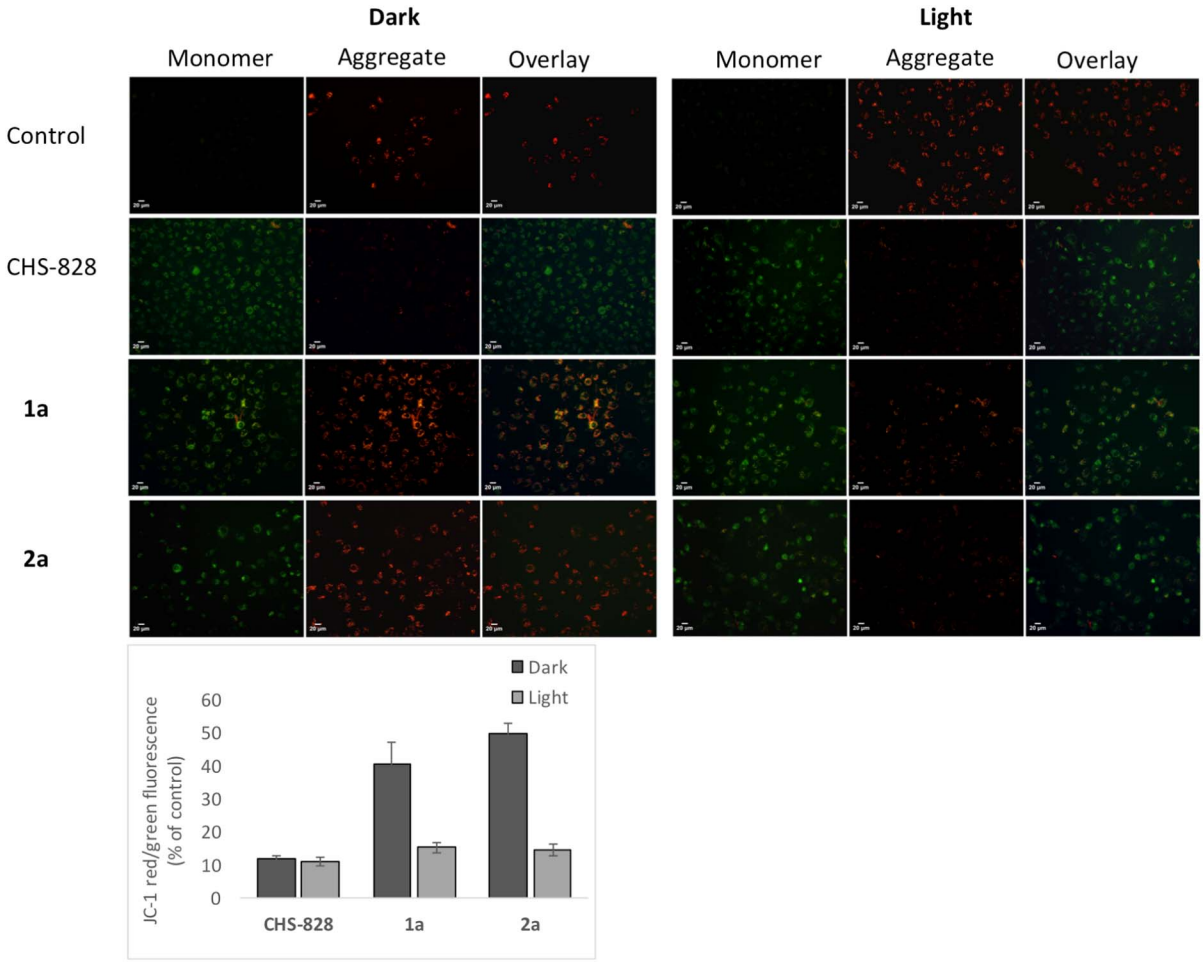


**Fig. 6.** Measurement of mitochondrial membrane potential. Ratio of red (aggregate) and green (monomer) fluorescence relative to untreated control cells of A549 cells treated with JC-1 after incubation with CHS-828, Complex (1a) or (2a) for 4 h Scale bar = 20 μm.

cells. Light irradiation did not alter ROS levels in either cells treated with CHS-828 or in the control cells. Complex (1a) or (2a) did not increase ROS levels with respect to the untreated control cells when incubated in the dark. When the cells were irradiated with light, however, a 4-fold increase was observed for each complex resulting in ROS levels similar to the CHS-828 treated cells. As neither Complex (1b) nor (2b) produce singlet oxygen when irradiated with light [31,32], this light-induced increase in ROS levels is most likely due to release of CHS-828.

### 3.8. Mitochondrial membrane potential ($\Delta\psi_m$)

In addition to increasing ROS levels, depletion of NAD + is known to decrease mitochondrial membrane potentials [33] and CHS-828 has previously been shown to decrease $\Delta\psi_m$ after long incubation periods [34]. $\Delta\psi_m$ was determined for cells treated with CHS-828, Complex (1a), and Complex (2a) for 4 h using the probe JC-1 by the ratio of red/green fluorescence. CHS-828 was found to significantly decrease $\Delta\psi_m$ (ca. 10 fold) with respect to the untreated control cells in both irradiated and non-irradiated cells (Fig. 6). Light irradiation did not significantly affect the red/green fluorescence ratio of cells treated with CHS-828, or the untreated control cells. In the dark, the ruthenium complexes had much a smaller effect on $\Delta\psi_m$ than CHS-828, reducing it by ca. 50% with respect to the control cells. The irradiated cells showed a significantly greater decrease in $\Delta\psi_m$, resulting in a $\Delta\psi_m$ comparable to cells treated with CHS-828. While a number of polypyridyl ruthenium complexes have been reported to accumulate in the mitochondria and induce apoptosis without light through depolarisation of the mitochondrial membrane [35–37], Complexes (1a) and (2a), do not markedly affect mitochondrial membrane function in the absence of light.

## 4. Conclusions

In combination, these results indicate that Complexes (1a) and (2a) can effectively deliver the cytotoxic ligand CHS-828 into tumour cells then release it with moderate doses of visible light. The marked increase in cytotoxicity, ROS levels, and depolarization of the mitochondrial membrane induced by irradiation of the complexes are consistent with photouncaging of CHS-828, though it cannot be completely discounted that excitation of the complexes themselves may also contribute to mitochondrial damage and/or ROS production. While Complexes (1a) and (2a) are still relatively cytotoxic in the dark, it is possible that this is due to a small amount of the cytotoxic CHS-828 ligand being released at concentrations too low to increase ROS levels. Given the very high accumulation of the complexes in tumour cells, the release of even a small percentage of the cytotoxic CHS-828 ligand would be expected to markedly influence $IC_{50}$ values.

In summary, we present a simple approach to reversibly modify the properties of a pyridine-containing cytotoxin. The ruthenium carrier systems have the potential to address the two major limitations of CHS-828, namely low bioavailability and non-selective toxicity. Both carriers combine water solubility with very high cellular accumulation, and are capable of reversibly deactivating this highly cytotoxic drug.

## Appendix A. Supplementary data

Supplementary data to this article can be found online at https://doi.org/10.1016/j.jinorgbio.2017.11.018.

## References


[1] J. Rautio, H. Kumpulainen, T. Heimbach, R. Oliyai, D. Oh, T. Jarvinen, J. Savolainen, Nat. Rev. Drug Discov. 7 (2008) 255.
[2] P. Klan, T. Solomek, C.G. Bochet, A. Blanc, R. Givens, M. Rubina, V. Popik, A. Kostikov, J. Wirz, Chem. Rev. 113 (2013) 119.
[3] S. Bonnet, Comments Inorg. Chem. 35 (2015) 179.
[4] J.D. Knoll, B.A. Albani, C. Turro, Acc. Chem. Res. 48 (2015) 2280.
[5] L. Zayat, C. Calero, P. Albores, L. Baraldo, R. Etchenique, J. Am. Chem. Soc. 125 (2003) 882.
[6] T. Respondek, R.N. Garner, M.K. Herroon, I. Podgorski, C. Turro, J.J. Kodanko, J. Am. Chem. Soc. 133 (2011) 17164.
[7] N. Karaoun, A.K. Renfrew, Chem. Commun. 51 (2015) 14038.
[8] A. Zamora, C.A. Denning, D.K. Heidary, E. Wachter, L.A. Nease, J. Ruiz, E.C. Glazer, Dalton Trans. 46 (2017) 2165.
[9] J.B.G.H. Chan, J. Wei, A.K. Renfrew, Eur. J. Inorg. Chem. 1679 (2017).
[10] M. Huisman, J.K. White, V.G. Lewalski, I. Podgorski, C. Turro, J.J. Kodanko, Chem. Commun. (Camb.) 52 (2016) 12590.
[11] A. Li, R. Yadav, J.K. White, M.K. Herroon, B.P. Callahan, I. Podgorski, C. Turro, E.E. Scott, J.J. Kodanko, Chem. Commun. (Camb.) 53 (2017) 3673.
[12] U.H. Olesen, M.K. Christensen, F. Bjorkling, M. Jaattela, P.B. Jensen, M. Sehested, S.J. Nielsen, Biochem. Biophys. Res. Commun. 367 (2008) 799.
[13] A. Garten, S. Schuster, M. Penke, T. Gorski, T. de Giorgis, W. Kiess, Nat. Rev. Endocrinol. 11 (2015) 535.
[14] H. Lovborg, J. Wojciechowski, R. Larsson, J. Wesierska-Gadek, Cancer Res. 62 (2002) 4206.
[15] B.M. Frost, G. Lonnerholm, P. Nygren, R. Larsson, E. Lindhagen, Anti-Cancer Drugs 13 (2002) 735.
[16] A. von Heideman, A. Berglund, R. Larsson, P. Nygren, Cancer Chemother. Pharmacol. 65 (2010) 1165.
[17] A. Ravaud, T. Cerny, C. Terret, J. Wanders, B.N. Bui, D. Hess, J.P. Droz, P. Fumoleau, C. Twelves, Eur. J. Cancer 41 (2005) 702.
[18] P. Hovstadius, R. Larsson, E. Jonsson, T. Skov, A.M. Kissmeyer, K. Krasilnikoff, J. Bergh, M.O. Karlsson, A. Lonnebo, J. Ahlgren, Clin. Cancer Res. 8 (2002) 2843.
[19] A. Bahreman, B. Limburg, M.A. Siegler, E. Bouwman, S. Bonnet, Inorg. Chem. 52 (2013) 9456.
[20] J.D. Knoll, B.A. Albani, C.B. Durr, C. Turro, J. Phys. Chem. A 118 (2014) 10603.
[21] L.P.A.C.M. Montalti, M.T. Gandolfi, Handbook of Photochemistry, Third edition, CRC Press, Florida, 2006.
[22] E. Binderup, F. Bjorkling, P.V. Hjarnaa, S. Latini, B. Baltzer, M. Carlsen, L. Binderup, Bioorg. Med. Chem. Lett. 15 (2005) 2491.
[23] A. Frei, R. Rubbiani, S. Tubafard, O. Blacque, P. Anstaett, A. Felgentrager, T. Maisch, L. Spiccia, G. Gasser, J. Med. Chem. 57 (2014) 7280.
[24] C. Tan, S. Lai, S. Wu, S. Hu, L. Zhou, Y. Chen, M. Wang, Y. Zhu, W. Lian, W. Peng, L. Ji, A. Xu, J. Med. Chem. 53 (2010) 7613.
[25] U. Schatzschneider, J. Niesel, I. Ott, R. Gust, H. Alborzinia, S. Wolfl, ChemMedChem 3 (2008) 1104.
[26] B. Siewert, V.H. van Rixel, E.J. van Rooden, S.L. Hopkins, M.J. Moester, F. Ariese, M.A. Siegler, S. Bonnet, Chemistry 22 (2016) 10960.
[27] J.H. Chern, K.S. Shia, C.M. Chang, C.C. Lee, Y.C. Lee, C.L. Tai, Y.T. Lin, C.S. Chang, H.Y. Tseng, Bioorg. Med. Chem. Lett. 14 (2004) 1169.
[28] S. Banerjee, P. Prasad, A. Hussain, I. Khan, P. Kondaiah, A.R. Chakravarty, Chem. Commun. (Camb.) 48 (2012) 7702.
[29] M.R. Gill, J.A. Thomas, Chem. Soc. Rev. 41 (2012) 3179.
[30] D. Cerna, H. Li, S. Flaherty, N. Takebe, C.N. Coleman, S.S. Yoo, J. Biol. Chem. 287 (2012) 22408.
[31] J.D. Knoll, B.A. Albani, C. Turro, Chem. Commun. (Camb.) 51 (2015) 8777.
[32] L.M. Loftus, J.K. White, B.A. Albani, L. Kohler, J.J. Kodanko, R.P. Thummel, K.R. Dunbar, C. Turro, Chemistry 22 (2016) 3704.
[33] C. Del Nagro, Y. Xiao, L. Rangell, M. Reichelt, T. O'Brien, J. Biol. Chem. 289 (2014) 35182.
[34] P. Martinsson, M. de la Torre, L. Binderup, P. Nygren, R. Larsson, Eur. J. Pharmacol. 417 (2001) 181.
[35] C. Tan, S. Wu, S. Lai, M. Wang, Y. Chen, L. Zhou, Y. Zhu, W. Lian, W. Peng, L. Ji, A. Xu, Dalton Trans. 40 (2011) 8611.
[36] V. Pierroz, T. Joshi, A. Leonidova, C. Mari, J. Schur, I. Ott, L. Spiccia, S. Ferrari, G. Gasser, J. Am. Chem. Soc. 134 (2012) 20376.
[37] L. Zeng, Y. Chen, J. Liu, H. Huang, R. Guan, L. Ji, H. Chao, Sci. Rep. 6 (2016) 19449.